www.nature.com/modpathol

ARTICLE

Immunohistochemical staining patterns of p53 predict the mutational status of *TP53* in oral epithelial dysplasia

Keisuke Sawada[1], Shuji Momose[1]✉, Ryutaro Kawano[1], Masakazu Kohda[2], Tarou Irié[3], Kenji Mishima[4], Takahiro Kaneko[5], Norio Horie[5], Yasushi Okazaki[2], Morihiro Higashi[1] and Jun-ichi Tamaru[1]

Next-generation sequencing of oral squamous cell carcinoma (OSCC) has revealed *TP53* as the most frequently mutated gene in OSCC mutually exclusive with human papillomavirus infection. Oral epithelial dysplasia (OED) is defined as a precancerous lesion of OSCC by the current World Health Organization (WHO) classification; therefore, it is assumed that *TP53* mutations occur in early precancerous conditions such as OED. Here, we conducted an integrated analysis of *TP53*, including whole coding sequencing of *TP53*, FISH analysis of the 17p13.1 locus, and immunohistochemical analysis for p53 (p53-IHC), in 40 OED cases. We detected 20 mutations in 16 (40%) OED cases, and four cases, each harbored two mutations. FISH analysis revealed six of 24 cases (25%) had a deletion on 17p13.1, and four cases had concurrent *TP53* mutations and 17p13.1 deletion (2-hit). Also, the increased frequency of *TP53* mutations in higher degrees of OED implies acquisition of the mutation is a major event toward OSCC. p53-IHC revealed that overall cases could be categorized into four patterns that correlate well with the mutational status of *TP53*. Especially, two patterns, broad p53 expression type (pattern HI) and p53 null type (pattern LS), strongly correlated with a missense mutation and nonsense mutation, respectively. Furthermore, seven of the 40 cases progressed to SCC, and six of these seven cases presented pattern HI or LS. Therefore, patterns HI and LS have a high risk for malignant transformation if excisional treatment is not performed irrespective of the dysplasia grade. Although the current WHO classification mainly focuses on morphological criteria for the diagnosis of OED, interobserver discrepancy appears in some instances of the OED diagnosis. Our immunohistochemical analysis supports a more accurate pathological diagnosis for OED in cases of low dysplastic changes or of differential diagnosis with non-dysplastic lesions.

Modern Pathology (2022) 35:177–185; https://doi.org/10.1038/s41379-021-00893-9

INTRODUCTION

Oral epithelial dysplasia (OED) is defined as "a spectrum of architectural and cytological epithelial changes caused by the accumulation of genetic changes" by the current WHO classification[1] and is a common manifestation of oral leukoplakia (OL)[1–3]. OED is further subclassified into three states: mild, moderate, and severe dysplasia[4].

The progression rate of OL in cases that exhibit OED at the time of biopsy into squamous cell carcinoma (SCC) is 6.6–53.2%[5–10]. Despite the precise criteria for OED, interobserver discrepancies may appear, because the pathological diagnosis of OED is based on morphological findings[11–13]. Though immunohistochemical staining for keratin 13 and keratin 17 for OED diagnosis is reported, immunohistochemical staining for OED diagnosis is not widely used in routine pathological practice[14–16].

Generally, most cancers, including oral squamous cell carcinoma (OSCC), acquire multiple genetic alterations to develop into a malignant state[17–19]. Next-generation sequencing (NGS) supports this observation[20–23], and *TP53* is the most frequent genetic alteration in head and neck squamous cell carcinoma (HNSCC) including OSCC. Interestingly, *TP53* mutations account for 60–80% of HNSCC and are mutually exclusive with human papillomavirus (HPV) infection. Furthermore, at 5%, the HPV infection rate in OSCC is much less than in other sites of HNSCC[23]. These results suggest that *TP53* mutations occur in the early stage of oral epithelial lesions including OED[20–25].

Although several reports studied the pathogenic role of *TP53* in OED by analyzing *TP53* mutations[26–29], the loss of heterozygosity (LOH) for the *TP53* locus[6,30,31], and immunohistochemistry (IHC)[32–35], no integrated analysis has examined the genetic alterations of p53, including mutations and LOH, and protein expression. Here, we conducted a *TP53* mutational screening by NGS, LOH screening of the *TP53* locus by fluorescence in situ hybridization (FISH) analysis, p53-IHC, and HPV-screening for OED to determine the genetic profile of the *TP53* status and clarify the OED pathogenesis at the molecular level.

MATERIALS AND METHODS

Patients

The study cohort consisted of 161 OL patients treated with biopsy or resection at the Department of Oral and Maxillofacial Surgery, Saitama

[1]Department of Pathology, Saitama Medical Center, Saitama Medical University, Saitama, Japan. [2]Diagnostics and Therapeutics of Intractable Diseases, Intractable Disease Research Center, Graduate School of Medicine, Juntendo University, Tokyo, Japan. [3]Division of Anatomical and Cellular Pathology, Department of Pathology, Iwate Medical University, Iwate, Japan. [4]Division of Pathology, Department of Oral Diagnostic Sciences, Showa University School of Dentistry, Tokyo, Japan. [5]Department of Oral and Maxillofacial Surgery, Saitama Medical Center, Saitama Medical University, Saitama, Japan. ✉email: momose@saitama-med.ac.jp

Received: 20 April 2021 Revised: 3 August 2021 Accepted: 4 August 2021
Published online: 17 August 2021

Table 1. OED patient characteristics ($n = 40$).

Age (y)	≤49	8
	50–59	10
	60–69	10
	70–79	10
	≥80	2
Gender	Female	15
	Male	25
Primary site	Tongue	31
	Gingiva	6
	Buccal mucosa	3
Tumor size (mm)	<20	32
	≥20	8
Dysplasia grade	mild	21
	moderate	13
	severe	6

OED oral epithelial dysplasia.
Tumor size clinical maximum diameter.

Medical Center, Saitama Medical University, between January 2000 and March 2018. These 161 cases were reviewed by four pathologists (K.S., S.M., R.K., and T.I.), who reclassified the grade of dysplasia according to the WHO Classification of Head and Neck Tumors (2017) to exclude non-neoplastic lesions and carcinoma in situ (CIS). We retrieved patient information from the medical records for all 40 OED patients of whom we analyzed the *TP53* mutation, LOH status of the *TP53* locus, and p53-IHC (Table 3). The present study was approved by the Institutional Review Board of Saitama Medical Center (No 1967) and conducted in accordance with the Declaration of Helsinki. Supplementary Figure 1 shows the schematic workflow, and Table 1 shows the patient data to which NGS was applied.

Sample preparation and DNA extraction

Formalin-fixed, paraffin-embedded (FFPE) specimens of 70 selected OED cases were sliced, and the tumor lesions of OED and non-neoplastic lesions were separated by laser capture microdissection using a PALM Microbeam, an Axio Observer Z1 fluorescence microscope, and PALM Robosoftware (ZEISS, Overkochen, Germany) if the OED was less than 20 mm^2. Lesions larger than 20 mm^2 were separated under the microscope using a scalpel. Then, genomic DNAs were extracted from deparaffinized FFPE tissue sections using an AllPrep DNA/RNA FFPE Kit (QIAGEN, Hilden, Germany), and the concentration of DNA was calculated using a Qubit® 3.0 Fluorometer and Qubit® dsDNA HS Assay Kit (Thermo Fisher Scientific, Waltham, MA, USA). Because 30 cases were excluded due to an insufficient amount or poor quality of DNA, we analyzed 40 OED cases.

TP53-targeted NGS and Sanger validation

We conducted *TP53*-targeted NGS using MiSeq (Illumina, San Diego, CA, USA) and the extracted genomic DNA from FFPE. To prepare the *TP53*-targeted library, we used an Accel-Amplicon Plus Comprehensive TP53 Panel (Swift Biosciences, Ann Arbor, MI, USA) that covers the whole coding sequence (exons 2-11) of *TP53*. After sequencing, the single nucleotide variants (SNVs) detected by NGS were validated by Sanger sequencing on an Applied Biosystems 3500/3500xL Genetic Analyzer and ABI Sequencing Analysis 5.1 software (Thermo Fisher Scientific). The used primer sets were referred to the IARC TP53 Database (http://p53.iarc.fr/ProtocolsAndTools.aspx) and are shown in Supplementary Table 1.

Bioinformatic analysis and annotation of *TP53* mutations

After NGS, a raw sequence read analysis was performed using our original bioinformatics pipeline[36]. The raw sequence read data passed the quality checks in FastQC (http://www.bioinformatics.babraham.ac.uk/projects/fastqc). Read trimming via base quality was performed using Trimmomatic-0.38[37]. Read alignments to the humanG1Kv37 reference genome (human_g1k_v37.fasta) were done using Burrows-Wheeler Aligner (BWA)[38]. PCR duplicate reads were removed using Picard, primer sequences were removed by soft-clipping on aligned SAM using Primerclip (https://swiftbiosci.com/biofx/), and non-mappable reads were removed using SAMtools[39]. After filtering out those reads, we applied GATK[40] and LoFreq[41] to perform base quality score recalibration and variant calling. Detected variants were annotated using ANNOVAR. The pipelines and filtering workflow used in this study are shown in Supplementary Figures 2 and 3, respectively. For the *TP53* mutations found in OEDs, mutation annotation was performed by searching for *TP53* variations in the IARC TP53 Database (http://p53.iarc.fr/TP53GeneVariations.aspx) and Gene Detail in CKB CORE (https://ckb.jax.org/gene/).

HPV-screening

The presence of HPV was screened using a previously described primer set and aliquots of DNA from the 40 OED samples (Supplementary Table 1)[42,43]. The amplification and PCR cycling conditions are previously described[44].

Immunohistochemistry for p53

The IHC staining of p53 was performed for the 40 OED cases in FFPE tissue sections using a BenchMark ULTRA (Ventana, Oro Valley, AZ, USA) and the PAb 1801 clone of p53 (abcam, Cambridge, UK).

FISH analysis for *TP53* gene (chromosome 17p13.1)

FISH analysis for *TP53* in FFPE specimens was also performed for the 40 OED cases. The *TP53* locus was detected using BAC clone RP1-89K1 (GenoTechs, Japan) labeled with spectrum orange along with Vysis CEP17 SpectrumAqua (Abbott Laboratories, Abbott Park, IL, USA). DNA labeling was performed using the Nick Translation System (Invitrogen, Tokyo, Japan). After hybridization, FISH images were scanned using BioView Soloweb (BioView Inc., Israel). FISH analysis of the *TP53* gene status was done as previously described[45]. In brief, the ratio of the *TP53* signal (orange) to the centromere 17 signal (aqua) was calculated by counting at least 100 tumor cells. A ratio lower than 0.81 indicated *TP53* deletion.

Data analysis from TCGA for *TP53*

Publicly available data for the *TP53* status in HNSCC were obtained from TCGA (https://www.cbioportal.org/study/summary?id = hnsc_tcga_pan_can_atlas_2018). Evaluation of the *TP53* copy number variation (CNV) status using Affymetrix SNP6 arrays for the TCGA HNSCC dataset (523 cases) was done following a previous report[46]. The CNV status is defined as segments with log2 fold change (LFC) values less than −0.25, which allows for the detection of single-copy CNVs.

Statistical analysis

All analyses were performed using EZR (Saitama Medical Center, Jichi Medical University, ver.1.33), and statistical significance was defined as a P value < 0.05[47].

RESULTS

TP53 mutational analysis and its functional significance

In total, 1822 *TP53* variants were detected in the 40 OED cases. Filtering for low allele frequency (<1%; i.e., sequence noise) removed 1357 variants, leaving 465 variants for the analysis. An additional filtering for false positives based on coverage of less than 400 variants and an allele frequency of less than 5% resulted in the identification of 47 variants. Another 27 variants were removed due to no pathogenic significance based on NCBI's Clinvar (https://www.ncbi.nlm.nih.gov/clinvar/). Finally, 20 *TP53* mutations were identified (Supplementary Figure 3).

Among the 40 analyzed cases, we detected 16 cases that had mutations in *TP53*, four of which harbored two mutations each (Table 2). The most frequent mutation type was a missense mutation (12/20, 60%), followed by a nonsense mutation (6/20, 30%), frameshift mutation (1/20, 5%), and splice site mutation (1/20, 5%) (Fig. 1A). These mutations were mainly located in the DNA-binding domain (DBD) (14/20), but four mutations were in the C-terminal domain, and one mutation each in either the N-terminal domain or the tetramerization domain (Fig. 1B and D). The *TP53* mutations at codons 245, 249, 273, and 282

Table 2. *TP53* mutations in OED.

Case No.	Position	Coding	Amino acid (protein)	Type	CLNSIG	VAF (%)	Sanger validation
6	7577560	c.721 T>C	p.S241P	SNV	Likely_pathogenic	13.9	+
12	7577111	c.825_826delTG	p.A276fs*29	INDEL	N/A	66.4	+
16	7577573	c.708 C>A	p.Y236*	SNV	N/A	10.2	N/D
24	7577509	c.772 G>C	p.E258Q	SNV	N/A	32.8	+
37	7578492	c.438 G>A	p.W146*	SNV	Pathogenic	17.5	+
40	7577022	c.916 C>T	p.R306*	SNV	Pathogenic	50.8	+
	7579882	c.31 G>C	p.E11Q	SNV	Conflicting_interpretations_of_pathogenicity	79.1	+
41	7574034	c.994-1 G>A	p.? (Unknown)	SNV	Pathogenic	27.0	+
	7577548	c.733 G>A	p.G245S	SNV	Pathogenic	26.1	N/D
42	7577120	c.818 G>T	p.R273L	SNV	Pathogenic	7.9	N/D
45	7578266	c.583 A>T	p.I195F	SNV	Likely_pathogenic	19.6	+
51	7577058	c.880 G>T	p.E294*	SNV	Pathogenic	11.8	+
	7579317	c.370 T>G	p.C124G	SNV	Uncertain_significance	26.0	+
53	7577022	c.916 C>T	p.R306*	SNV	Pathogenic	22.0	+
55	7574018	c.1009 C>T	p.R337C	SNV	Pathogenic	36.6	+
58	7578413	c.517 G>T	p.V173L	SNV	Likely_pathogenic	43.2	+
63	7578392	c.538 G>T	p.E180*	SNV	N/A	10.4	N/D
	7578508	c.422 G>A	p.C141Y	SNV	Pathogenic/Likely_pathogenic	10.4	N/D
64	7577094	c.844 C>T	p.R282W	SNV	Pathogenic	28.8	+
67	7577536	c.745 A>G	p.R249G	SNV	Uncertain_significance	29.0	+

Position was referenced by Homo sapiens (human) genome assembly GRCh37/hg19.
Coding and amino acids were referred to accession mRNA sequence number NM_00546 and accession protein number NP_001119589.
N/A not available, *VAF* variant allele frequency, *N/D* not detected.

(NP_001119589) are reported as hotspot mutations in human cancers[48].

To predict the functional significance of the detected mutations, we applied two databases: the Search TP53 variation in the IARC TP53 Database and Gene Detail in CKB CORE. In the IARC TP53 Database, nine (50%) mutations were predicted to be nonfunctional, two (11.1%) mutations were partially functional, one (6%) mutation was functional, and six (33.3%) missense or nonsense mutations were not assigned to any category. According to CKB CORE, 13 (72.2%) mutations were predicted as nonfunctional, three (16.7%) mutations were unknown, and two (11.1%) mutations were not validated. These results were integrated and are shown in Fig. 1C.

Furthermore, the relationship between the frequency of *TP53* mutations and the degree of dysplasia was analyzed. The number of cases that had a mutation was five of 21 (23.8%) in mild dysplasia, seven of 13 (53.8%) in moderate dysplasia, and four of six (66.7%) in severe dysplasia. The higher the degree of dysplasia, the more frequently a *TP53* mutation was observed (Fig. 2).

Immunohistochemistry of p53 in OEDs

We performed IHC for p53 on all cases that had screened *TP53* mutations. After evaluation of the IHC results, we categorized the cases into four distinctive staining patterns. A schematic representation of these patterns and representative cases are shown in Fig. 3. Cases that had p53-positive cells scattered in the basal or parabasal layer were designated as pattern NM (Normal), and this pattern resembled the staining pattern of the normal oral mucosa (Fig. 3A). In the second pattern, the basal and parabasal layers were widely positive for p53, and we designated this pattern BP (Basal and Parabasal) (Fig. 3B). To discriminate patterns NM and BP, we set the cutoff value at 50% positivity for p53 (NM < 50%; BP ≥ 50%). The third pattern was diffusely positive for p53 more in the superficial layer than parabasal layer and designated as pattern HI (High) (Fig. 3C). The fourth pattern was a complete loss of p53 expression in the lesion and designated as pattern LS (Loss) (Fig. 3D). Based on these categories, 17 cases (42.5%) belonged to pattern NM, nine (22.5%) cases to pattern BP, eight (20%) cases to pattern HI, and six (15%) cases to pattern LS.

LOH of *TP53* (chromosome 17p13.1)

Among the 40 cases, 24 cases were successfully evaluated for the *TP53* locus status by FISH. The samples for the others were not enough or of low quality to obtain hybridization signals for more than 100 target cells. We found 6 cases (25%) had a deletion at the *TP53* locus (Fig. 4).

TP53 status in HNSCC from TCGA data

To analyze the *TP53* status in HNSCC, we searched TCGA for the frequency of *TP53* mutations (SNVs and small indels) and the LOH status in the *TP53* locus. In total, 523 cases were analyzed, and 415 cases were HPV-negative. Among the HPV-negative cases, 374 cases harbored *TP53* mutations and/or copy number aberrations (Supplementary Figure 4A and B, Supplementary Table 2). Structural aberrations of the *TP53* locus were also analyzed. We found the deletion of *TP53* in 25 of 97 cases that carry a truncated mutation (nonsense and frameshift mutation), one of eight cases that carry an in-frame mutation, two of 23 cases that carry a splice mutation, 44 of 172 cases that carry a missense mutation, and one of 41 cases that carry multiple mutations. Taken together, 73 of 415 (17.6%) HPV-negative cases carried a 2-hit (LOH and *TP53* mutation) for *TP53*.

Integrated genetic profile of *TP53* in OED

We integrated all the results (*TP53* mutation, HPV-screening, LOH status for *TP53*, and p53 expression analysis) and made a genetic profile for a comprehensive understanding of OED (Fig. 4).

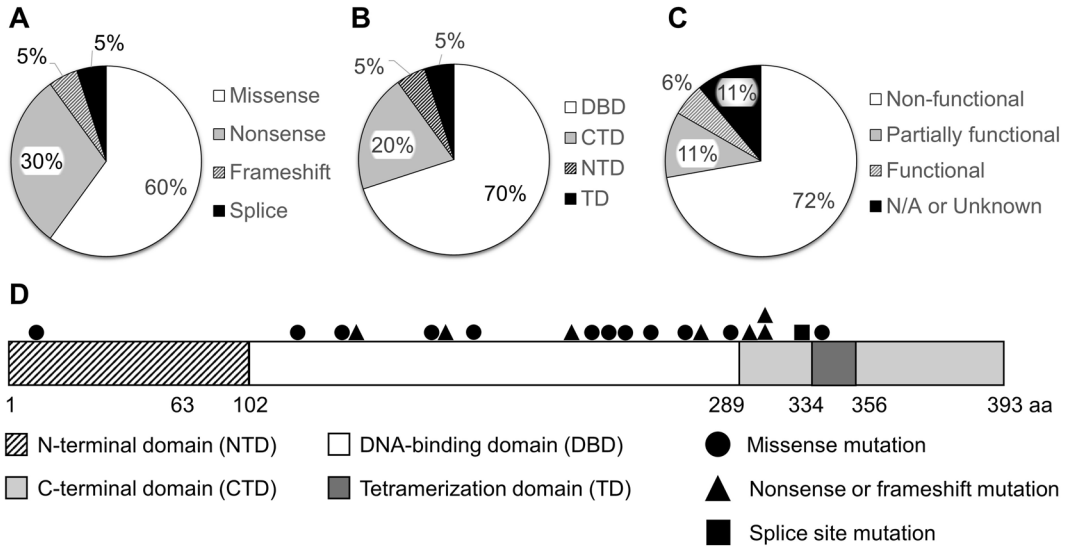

Fig. 1 Patterns of *TP53* mutations in 40 OED cases. Frequency of the mutation type (**A**), mutation distribution (**B**), and predicted effect of the mutation (**C**) in 40 OED cases. The predicted effect is shown by integrating the results of Search TP53 variation in the IARC TP53 Database and Gene Detail in CKB CORE. N/A, not available. NTD, N-terminal domain; DBD, DNA-binding domain; CTD, C-terminal domain; and TD, Tetramerization domain. **D** Schematic distribution of mutations in p53 (accession number NP_001119589).

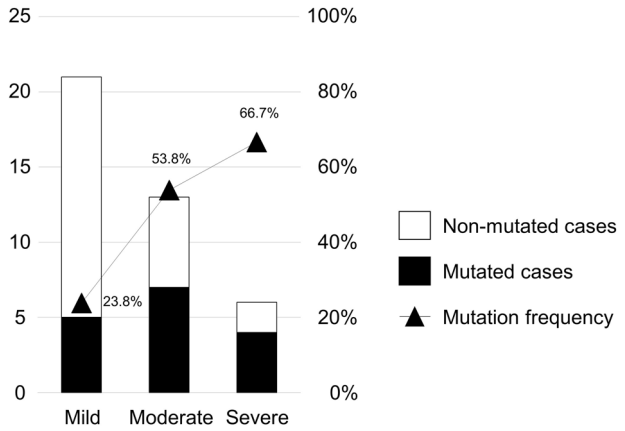

Fig. 2 Association of *TP53* mutation and dysplasia grade. The case number of each dysplastic grade according to the *TP53* mutation. The numbers on the left and right indicate the number of cases and mutation frequency (%), respectively.

Abnormal p53 expression patterns (patterns BP, HI, and LS) were significantly associated with the *TP53* mutations detected by NGS ($p = 0.0028$, Fisher's exact test). Especially, patterns HI and LS had *TP53* mutations in seven of eight cases (87.5%) and five of six cases (83.3%), respectively. However, there was no significant difference in the *TP53* mutation frequency between patterns NM and BP ($p = 0.59$, Fisher's exact test). When genomic and genetic aberrations of *TP53* obtained from FISH and NGS analyses were taken together, we found significant differences in the *TP53* mutation rates between pattern NM and abnormal patterns (patterns BP, HI, and LS) ($p = 0.0040$, Fisher's exact test). However, there was no significant difference in *TP53* aberrations between patterns NM and BP ($p = 0.171$, Fisher's exact test).

Because *TP53* is a tumor suppressor gene and 2-hit were observed in 17.6% (73/415) of HPV-negative OSCC from TCGA (Supplementary Table 2), we investigated the correlation between the degree of dysplasia and the genetic condition of *TP53* (monoallelic or biallelic aberrations) by examining *TP53* mutations and the LOH status of the *TP53* locus. From the integrated profile (Fig. 4), biallelic aberrations (*TP53* SNV and LOH) of *TP53* were observed in four of 24 (16.7%) cases. All four cases belonged to pattern HI, and the grade of dysplasia was moderate or severe (two cases each). Although another four cases had two mutations each, we could not distinguish whether the mutations exist in the same allele of chromosome 17.

Clinical outcomes with pathological and genetic findings in OED

We summarize the clinical outcomes of the 40 OED patients along with the pathological and genetic findings in Table 3. We obtained outcome data for 37 patients, seven of whom progressed to OSCC. Five of the patients who proceeded to SCC from OED were followed up without additional excisional treatment after biopsy based on the patients' choice. As for the other two patients, patient No. 37 underwent surgical excision after the biopsy, and the surgical margin was positive for dysplasia. However, the patient did not undergo further surgical treatment, and SCC was detected 12 months after the initial diagnosis. The second patient, patient No. 42, underwent surgical excision and complete resection. Under follow-up, the patient repeatedly underwent biopsies due to multiple OL lesions. After 158 months, SCC arose at the same site as the resected region. For the 30 patients who did not progress to SCC, three did not receive additional treatment during the follow-up after biopsy for the initial diagnosis of OED (one had mild dysplasia and the other two had moderate dysplasia). The one patient diagnosed with mild dysplasia underwent spontaneous regression of the lesion after follow-up (96 months). The two patients diagnosed with moderate dysplasia had a continuously stable disease state. As for the other 27 patients, no disease recurrence was observed after follow-up. All patients who progressed to SCC were either moderate dysplasia (four cases) or severe dysplasia (three cases), and none of the mild dysplasia cases proceeded to SCC.

With regards to the genetic findings, six of the seven cases that progressed to SCC were significantly associated with *TP53* aberrations either carrying *TP53* mutations and/or LOH at chromosome 17p13.1 ($p = 0.0422$, Fisher's exact test). Of the patients who progressed to SCC, three showed pattern HI, three showed pattern LS, and one showed pattern BP. Especially, the progression events of SCC were significantly associated with p53-IHC pattern HI or LS ($p = 0.0070$, Fisher's exact test). Combining the p53-IHC pattern and *TP53* aberration observations, all patients

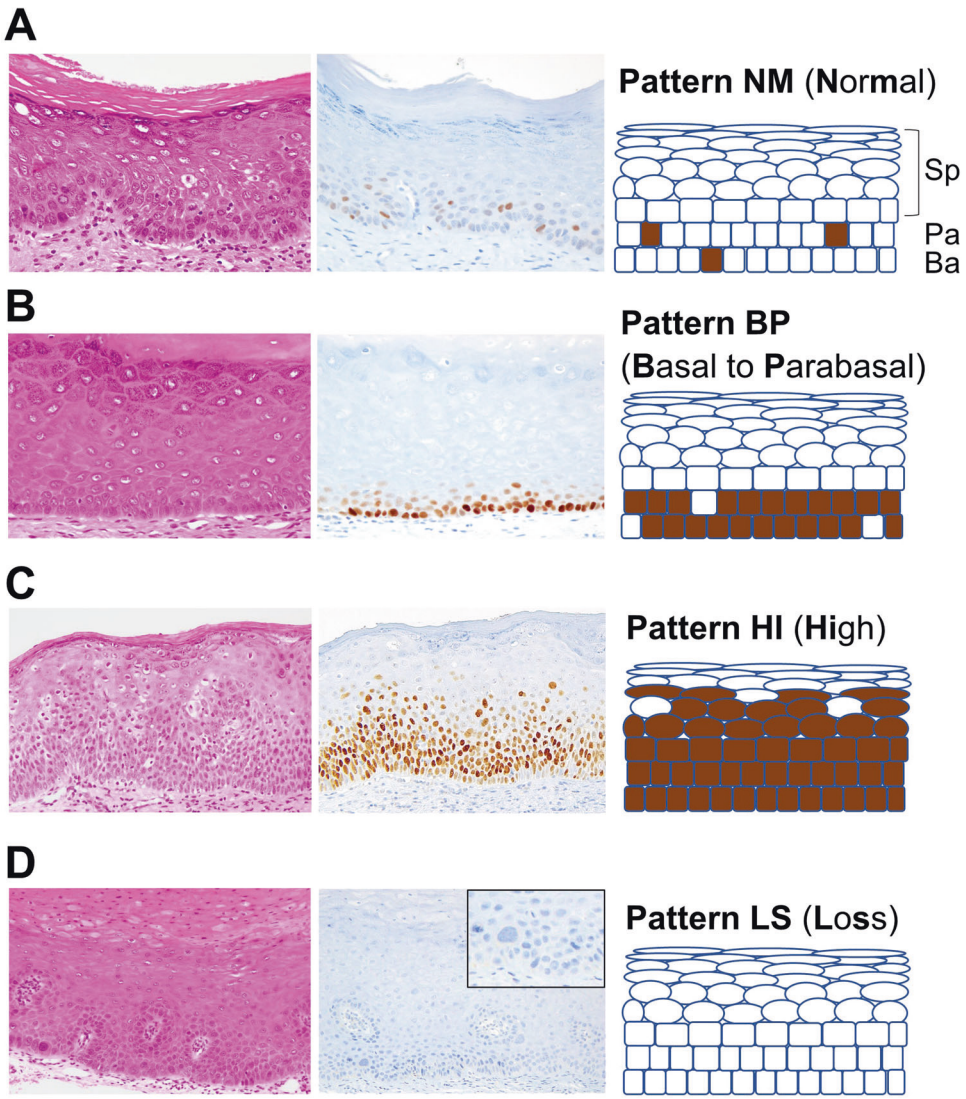

Fig. 3 p53-IHC staining patterns and schemas of OED. Representative immunohistochemical staining results (20X) and schemas for the 4 detected patterns. **A** Pattern NM: p53-positive cells are scattered in the basal or parabasal layer (normal staining pattern of the oral mucosa). **B** Pattern BP: p53-positive cells are widely diffusive in the basal and parabasal layers. **C** Pattern HI: p53-positive cells are broadly distributed in more than three layers. **D** Pattern LS: the expression of p53 is regionally absent. The inset shows a high magnification of the basal layer area. Sp, Pa, and Ba indicate spinous layer, parabasal layer, and basal layer, respectively.

who progressed to SCC had p53-IHC pattern HI or LS and/or *TP53* aberrations ($p = 0.0058$, Fisher's exact test).

DISCUSSION

A diagnosis of OED is mainly made by morphological findings based on hematoxylin-eosin staining, with additional immunohistochemical staining done in some instances. Although the WHO provides diagnostic criteria for OED, the reproducibility for grading or differential diagnosis with a reactive lesion is not reliable[11–13]. Woo et al.[49] suggested the term "keratosis of unknown significance (KUS)" for lesions that are not cytologically dysplastic and not reactive. The notion of KUS representing a very early dysplasia that also has the potential to develop into invasive SCC may explain the transition between reactive atypia and mild dysplasia. However, both KUS and OED are diagnosed by morphological criteria. Objective information that predicts the clinical outcome is desired to improve the diagnosis of OED and related disease entities.

A recent large genetic cohort series that analyzed HNSCC including OSCC revealed that *TP53* is the most frequently mutated gene[20–25]. Therefore, we hypothesized that *TP53* mutations occur in the early lesion of OSCC as the founder event and that analyzing *TP53* in OED may provide a better understanding of the pathology and lead to a more precise diagnosis. In the present study, we analyzed 40 OED cases by NGS and IHC and found four distinct p53 staining patterns that correlated with *TP53* mutations (Figs. 3 and 4). Because patterns HI and LS had a high mutational rate of *TP53*, cases with these patterns may be diagnosed as OED based not only on morphological atypia but also by the accumulation of genetic changes even if a case presents low dysplastic change and has difficult diagnosis. Most cases that progressed to SCC from OED were pattern HI or LS, except for one case that presented pattern BP. Based on the clinical information of the six patients who were initially diagnosed with OED but progressed to SCC without further treatment, p53-IHC patterns HI and LS strongly indicated the need for further excisional treatment of residual lesions. In contrast, pattern NM contained a low *TP53*

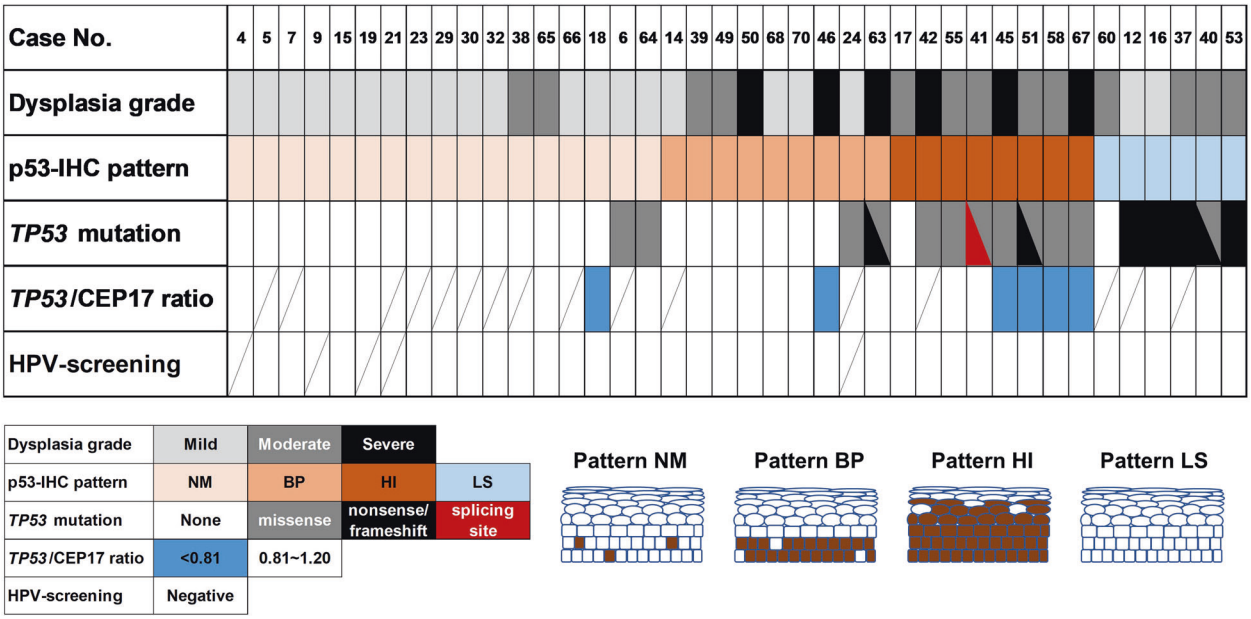

Fig. 4 Integrated *TP53* gene profiles of 40 OED cases. Dysplasia grade, p53-IHC pattern, mutation type of *TP53*, FISH results for *TP53* locus, and HPV status are colored by the column indicated in the left lower side. Small schemas for each p53-IHC pattern are indicated at the right lower side.

mutation rate (2/17, 11.8%), and pattern BP had a mutation rate of *TP53* that was between pattern NM and patterns HI and LS (2/9, 22.2%). Although only two of the 14 cases that presented p53-IHC pattern NM had follow-up after the biopsy without excisional treatment, these two cases were complete regression or persistent disease state. Thus, pattern NM indicates a low *TP53* mutation rate and good prognosis. However, the number of cases that were followed for a long time without excisional treatment after biopsy was small in our cohort. A larger cohort should be used to investigate the relationship between p53-IHC patterns and clinical outcomes of OEDs.

Previous studies found that an OED lesion with dysplastic changes reveals spontaneous regression in some instances[50,51]. From our analysis, OED with low-grade dysplasia carries a low *TP53* mutational incidence, and one patient (No.7) in this study who was examined by biopsy only without further treatment was diagnosed as mild dysplasia and revealed to have no *TP53* mutation and p53-IHC pattern NM. This case presented spontaneous regression, suggesting no founder mutation, similar to cases with *TP53* aberrations in OED, and thus lacks the self-autonomous potential capable of progressing to OSCC and may instead finally lead to regression. Overall, cases that manifest both mild dysplastic changes and p53-IHC pattern NM may include both reactive lesions with atypia and OED with mild atypia. Therefore, it is difficult to correctly diagnose these cases, resulting in inter-examiner variability in some instances.

Although several studies have analyzed the relationship between *TP53* mutations and the dysplastic grade of OED, no significant correlation has been established due to the small number of analyzed cases[26–29,33,52,53] (Supplementary Table 3). Furthermore, IHC patterns were not taken into account in some studies. Cruz et al.[52] presented three p53-IHC patterns: no expression, confined to the basal cell layer, and clear suprabasal layer. The suprabasal layer pattern corresponds to pattern HI in our cohort. Although it is easy to imagine that our pattern LS corresponds to the no expression pattern, pattern NM in our criteria may also correspond to this pattern, because the negative pattern included a pathology diagnosis of both "normal" and "premalignant lesions". Another reason is that pattern NM exhibits a scattered or even weak staining pattern, which is identical to the non-inflammatory normal epithelium of oral mucosa. Kushner et al.[33] defined four patterns that show similarity with our patterns. Although the "no staining pattern" defined by Kushner et al. corresponds to our pattern LS, their scattered pattern seems to include both patterns NM and BP, and their diffuse and compact patterns seem to correspond with pattern HI. We also observed a case resembling the compact pattern described by Kushner et al. This case presented p53-positive cells above the parabasal layer, consistent with pattern HI.

Two representative antibodies against p53 protein are used for IHC analysis in daily routine practice: DO-7 and PAb 1801. Both recognize the N-terminal region of p53, and the epitope regions for DO-7 and PAb 1801 correspond to 20-25 aa and 46-53 aa, respectively. Because *TP53* mutations mainly occur in the DBD domain (102-289 aa) and mutations in the N-terminal region are rare, both antibodies react with p53 protein irrespective of the mutation. In addition, in a previous study analyzing 245 cases of breast cancer[54] and 67 cases of HNSCC[55], there was no significant difference in the sensitivity or specificity between the two monoclonal antibodies against p53. Additionally, Lavieille et al.[55] examined the relationship between *TP53* mutations and IHC, finding no difference in the staining irrespective of the *TP53* mutation. Therefore, our data are comparable with previous p53-IHC studies in OEDs.

We analyzed 40 OED cases and revealed that the higher the grade of dysplasia, the more *TP53* mutations are observed (Fig. 2). Thus, *TP53* mutations are a common event in the later stage of OED, an observation also described by Shahnavaz et al.[27]. These findings support the dysfunction of *TP53* being a strong oncogenic driver toward OSCCs. From previous studies[26–29], the most frequently mutated domain of *TP53*, DBD (exons 5-8), is the main target when searching for OED mutations (Supplementary Table 3). In this study, we screened the whole exons of *TP53* by NGS, detecting six of 20 (30%) mutations outside the DBD. Indeed, we found that five of 16 cases (31.3%) that showed mutations outside the DBD had not previously been searched by Sanger sequencing, demonstrating that the actual frequency of *TP53* mutations is higher than previously reported. However, several cases had neither *TP53* aberration (SNV and LOH) nor HPV infection in our cohort (22/40, 55%). Villa et al.[56] reported that

Table 3. Clinical outcomes and pathological and genetic findings of the 40 OED patients.

Case No.	Age (y)	Gender	Primary site	Tumor size (max. diameter, mm)	Procedure for the diagnosis	Diagnosis	Treatment after diagnosis	Follow-up (months)	Outcome	*TP53* mutation	LOH (17p13.1)	*TP53* abberation[b]	p53-IHC pattern[c]
4	67	F	T	4	Excisional biopsy	Mi	No	60	DF	–	–	–	NM
5	45	M	T	13	Biopsy	Mi	Resection	193	DF	–	N/D	–	NM
6	59	F	T	4	Excisional biopsy	Mi	No	159	DF	+	N/D	+	NM
7	57	F	T	8	Biopsy	Mi	Follow-up	96	Complete regression	–	N/D	–	NM
9	59	F	T	3	Excisional biopsy	Mi	No	Unknown	Unknown	–	–	–	NM
12	62	F	T	13	Biopsy	Mi	Resection	90	DF	+	N/D	+	LS
14	39	M	T	9	Excisional biopsy	Mi	No	89	DF	–	N/D	_	BP
15	71	F	T	12	Biopsy	Mi	Resection	60	DF	–	–	–	NM
16	55	M	T	10	Excisional biopsy	Mi	No	3	DF	+	–	+	LS
17	63	M	G	15	Biopsy	Mo	Resection	15	DF	–	–	–	HI
18	61	M	T	20	Biopsy	Mi	Resection	47	DF	–	+	+	NM
19	60	M	T	6	Biopsy	Mi	No	Unknown	Unknown	–	–	–	NM
21	56	M	G	3	Biopsy	Mi	No	Unknown	Unknown	–	N/D	–	NM
23	34	M	T	10	Excisional biopsy	Mi	No	128	DF	–	N/D	–	NM
24	59	M	T	7	Excisional biopsy	Mi	No	111	DF	+	N/D	+	BP
29	21	M	T	5	Excisional biopsy	Mi	No	12	DF	–	N/D	–	NM
30	55	M	T	8	Biopsy	Mi	Resection	3	DF	–	N/D	–	NM
32	68	M	G	16	Excisional biopsy	Mi	No	48	DF	–	N/D	–	NM
37	32	F	T	12	Biopsy	Mo	Resection[a]	12	Relapse as SCC	+	N/D	+	LS
38	76	M	G	7	Excisional biopsy	Mo	No	58	DF	–	N/D	–	NM
39	60	M	T	7	Excisional biopsy	Mo	No	74	DF	–	–	–	BP
40	79	M	T	21	Biopsy	Mo	Follow-up	48	Progression to SCC	+	–	+	LS
41	54	M	T	12	Biopsy	Mo	Follow-up	79	Persistent OL	+	–	+	HI
42	49	F	B	15	Biopsy	Se	Resection	158	Relapse of SCC	+	N/D	+	HI
45	55	M	T	25	Biopsy	Se	Resection	99	DF	+	+	+	HI
46	72	F	B	30	Biopsy	Se	Follow-up	9	Progression to SCC	–	+	+	BP
49	76	M	T	14	Biopsy	Mo	Resection	44	DF	–	–	–	BP
50	66	M	G	8	Excisional biopsy	Se	No	28	DF	–	–	–	BP
51	65	M	T	8	Biopsy	Mo	Resection	24	DF	+	+	+	HI
53	43	M	T	15	Biopsy	Mo	Resection	33	DF	+	–	+	LS
55	59	F	T	6	Excisional biopsy	Mo	No	45	DF	+	–	+	HI
58	49	M	T	40	Biopsy	Mo	Follow-up	2	Progression to SCC	+	+	+	HI
60	64	F	T	25	Biopsy	Mo	Follow-up	24	Progression to SCC	–	N/D	–	LS
63	76	F	T	7	Biopsy	Se	Resection	16	DF	+	–	+	BP
64	80	M	T	12	Excisional biopsy	Mi	No	34	DF	+	–	+	NM
65	81	F	B	10	Biopsy	Mo	Follow-up	37	Persistent OL	–	–	–	NM
66	76	F	T	20	Biopsy	Mi	Resection	24	DF	–	N/D	–	NM
67	77	M	G	20	Biopsy	Se	Follow-up	12	Progression to SCC	+	+	+	HI
68	75	F	T	8	Excisional biopsy	Mi	No	28	DF	–	–	–	BP
70	75	M	T	12	Biopsy	Mi	Resection	36	DF	–	–	–	BP

F female, *M* male, *T* tongue, *G* gingiva, *B* buccal mucosa, *Mi* mild dysplasia, *Mo* moderate dysplasia, *Se* severe dysplasia, *DF* disease free, *SCC* squamous cell carcinoma, *OL* oral leukoplakia, *LOH* loss of heterozygosity, *N/D* not detected.

[a]Surgically resected (surgical margins were positive for dysplasia) and follow up.

[b]The abberation of *TP53* has *TP53* mutation and/or LOH (17p13.1).

[c]The pattern of p53-IHC corresponds to Fig. 3.

KMT2C is the most frequently mutated gene in early oral intraepithelial lesions, such as OED and KUS. Though this result may explain the cases that had neither *TP53* mutation nor HPV infection, the study did not screen for HPV infection in those cases. Furthermore, previous mutations found no recurrent *KMT2C* mutation in OSCC[22–24]. While *KMT2C* mutation may represent a genetic alteration of early oral intraepithelial lesions, further study is needed to clarify the multistep carcinogenesis toward OSCC.

FISH analysis revealed six cases presenting 17p13.1 deletion, two of which have no *TP53* mutation based on NGS. These two cases presented patterns NM or BP. The other four cases presented pattern HI. The IHC data is thought to reflect the stability of p53 protein, which depends on various aberrations, but mainly missense and nonsense *TP53* mutations[57,58]. Based on the IHC patterns, we considered that cases with 17p13.1 deletion only are milder compared to cases with *TP53* mutations. Consistently, the overall survival of acute myelogenous leukemia patients is longer in cases with deletion of the *TP53* locus only compared with the deletion and *TP53* mutations[59]. This result supports the functional and clinical consequences of observing the mutations and allelic status of *TP53*. Moreover, the higher frequency of *TP53* mutations only compared with 17p13.1 loss only implies *TP53* mutations occur prior to 17p13.1 loss including *TP53* LOH.

To conclude, in this study, we performed an integrated analysis of the *TP53* gene in OED and clarified the relationship between the genetics status of *TP53* and the interpretation of IHC for p53. Although the current WHO classification mainly focuses on morphological criteria for the diagnosis of OED, we recommend additional IHC analysis of *TP53* for accurate pathological diagnosis.

DATA AVAILABILITY

All data generated or analyzed during this study are included in this published article.

REFERENCES

1. El-Naggar, A. K., Chan, J. K., Grandis, J. R., Takata, T., Slootweg, P. J. *WHO classification of head and neck tumours*. International Agency for Research on Cancer (2017).
2. Warnakulasuriya, S., Johnson, N. W. & Van Der Waal, I. Nomenclature and classification of potentially malignant disorders of the oral mucosa. *J Oral Pathol Med* **36**, 575–80 (2007).
3. Speight, P. M. Update on oral epithelial dysplasia and progression to cancer. *Head Neck Pathol* **1**, 61–66 (2007).
4. Warnakulasuriya, S., Reibel, J., Bouquot, J. & Dabelsteen, E. Oral epithelial dysplasia classification systems: predictive value, utility, weaknesses and scope for improvement. *J Oral Pathol Med* **37**, 127–33 (2008).
5. Schepman, K. P., van der Meij, E. H., Smeele, L. E. & Van Der Waal, I. Malignant transformation of oral leukoplakia: a follow-up study of a hospital-based population of 166 patients with oral leukoplakia from The Netherlands. *Oral Oncol* **34**, 270–5 (1998).
6. Rosin, M. P., Cheng, X., Poh, C., Lam, W. L., Huang, Y. & Lovas, J. et al. Use of allelic loss to predict malignant risk for low-grade oral epithelial dysplasia. *Clin Cancer Res* **6**, 357–62 (2000).
7. Brouns, E., Baart, J., Karagozoglu, K., Aartman, I., Bloemena, E. & Van Der Waal, I. Malignant transformation of oral leukoplakia in a well-defined cohort of 144 patients. *Oral Dis* **20**, e19–e24 (2014).
8. Wang, Y.-Y., Tail, Y.-H., Wang, W.-C., Chen, C.-Y., Kao, Y.-H. & Chen, Y.-K. et al. Malignant transformation in 5071 southern Taiwanese patients with potentially malignant oral mucosal disorders. *BMC Oral Health* **14**, 99 (2014).
9. Chaturvedi, A. K., Udaltsova, N., Engels, E. A., Katzel, J. A., Yanik, E. L. & Katki, H. A. et al. Oral leukoplakia and risk of progression to oral cancer: a population-based cohort study. *J Natl Cancer Inst* **112**, 1047–54 (2020).
10. Lee, J. J., Hung, H. C., Cheng, S. J., Chen, Y. J., Chiang, C. P. & Liu, B. Y. et al. Carcinoma and dysplasia in oral leukoplakias in Taiwan: prevalence and risk factors. *Oral Surg Oral Med Oral Pathol Oral Radio Endod* **101**, 472–80 (2006).
11. Abbey, L. M., Kaugars, G. E., Gunsolley, J. C., Burns, J. C., Page, D. G. & Svirsky, J. A. et al. Intraexaminer and interexaminer reliability in the diagnosis of oral epithelial dysplasia. *Oral Surg Oral Med Oral Pathol Oral Radio Endod* **80**, 188–91 (1995).
12. Karabulut, A., Reibel, J., Therkildsen, M. H., Praetorius, F., Nielsen, H. W. & Dabelsteen, E. Observer variability in the histologic assessment of oral premalignant lesions. *J Oral Pathol Med* **24**, 198–200 (1995).
13. Fischer, D. J., Epstein, J. B., Morton, T. H. & Schwartz, S. M. Interobserver reliability in the histopathologic diagnosis of oral pre-malignant and malignant lesions. *J Oral Pathol Med* **33**, 65–70 (2004).
14. Ida-Yonemochi, H., Maruyama, S., Kobayashi, T., Yamazaki, M., Cheng, J. & Saku, T. Loss of keratin 13 in oral carcinoma in situ: a comparative study of protein and gene expression levels using paraffin sections. *Mod Pathol* **25**, 784–94 (2012).
15. Nobusawa, A., Sano, T., Negishi, A., Yokoo, S. & Oyama, T. Immunohistochemical staining patterns of cytokeratins 13, 14, and 17 in oral epithelial dysplasia including orthokeratotic dysplasia. *Pathol Int* **64**, 20–7 (2014).
16. Wils, L. J., Poell, J. B., Evren, I., Koopman, M. S., Brouns, E. R. E. A. & De Visscher, J. G. A. M. et al. Incorporation of differentiated dysplasia improves prediction of oral leukoplakia at increased risk of malignant progression. *Mod Pathol* **33**, 1033–40 (2020).
17. Califano, J., van der Riet, P., Westra, W., Nawroz, H., Clayman, G. & Piantadosi, S. et al. Genetic progression model for head and neck cancer: implications for field cancerization. *Cancer Res* **56**, 2488–92 (1996).
18. Tabor, M. P., Brakenhoff, R. H., van Houten, V. M., Kummer, J. A., Snel, M. H. & Snijders, P. J. et al. Persistence of genetically altered fields in head and neck cancer patients: biological and clinical implications. *Clin Cancer Res* **7**, 1523–32 (2001).
19. Braakhuis, B. J. M. A genetic explanation of slaughter's concept of field cancerization: evidence andclinical implications1. *Cancer Res* **63**, 1727–30 (2003).
20. Stransky, N., Egloff, A. M., Tward, A. D., Kostic, A. D., Cibulskis, K. & Sivachenko, A. et al. The mutational landscape of head and neck squamous cell carcinoma. *Science* **333**, 1157–60 (2011).
21. Cancer Genome Atlas Network. Comprehensive genomic characterization of head and neck squamous cell carcinomas. *Nature* **517**, 576–82 (2015).
22. Pickering, C. R., Zhang, J., Yoo, S. Y., Bengtsson, L., Moorthy, S. & Neskey, D. M. et al. Integrative genomic characterization of oral squamous cell carcinoma identifies frequent somatic drivers. *Cancer Disco* **3**, 770–81 (2013).
23. Gillison, M. L., Akagi, K., Xiao, W., Jiang, B., Pickard, R. K. L. & Li, J. et al. Human papillomavirus and the landscape of secondary genetic alterations in oral cancers. *Genome Res* **29**, 1–17 (2019).
24. Nakagaki, T., Tamura, M., Kobashi, K., Koyama, R., Fukushima, H. & Ohashi, T. et al. Profiling cancer-related gene mutations in oral squamous cell carcinoma from Japanese patients by targeted amplicon sequencing. *Oncotarget* **8**, 59113–22 (2017).
25. Nakagaki, T., Tamura, M., Kobashi, K., Omori, A., Koyama, R. & Idogawa, M. et al. Targeted next-generation sequencing of 50 cancer-related genes in Japanese patients with oral squamous cell carcinoma. *Tumour Biol* **40**, 101042831880018 (2018).
26. Kusama, K., Okutsu, S., Takeda, A., Himiya, T., Kojima, A. & Kidokoro, Y. et al. p53 gene alterations and p53 protein in oral epithelial dysplasia and squamous cell carcinoma. *J Pathol* **178**, 415–21 (1996).
27. Shahnavaz, S. A., Regezi, J. A., Bradley, G., Dubé, I. D. & Jordan, R. C. p53 gene mutations in sequential oral epithelial dysplasias and squamous cell carcinomas. *J Pathol* **190**, 417–22 (2000).
28. Ogmundsdottir, H. M., Bjornsson, J. & Holbrook, W. P. Role of TP53 in the progression of pre-malignant and malignant oral mucosal lesions. A follow-up study of 144 patients. *J Oral Pathol Med* **38**, 565–71 (2009).
29. Graveland, A. P., Bremmer, J. F., De Maaker, M., Brink, A., Cobussen, P. & Zwart, M. et al. Molecular screening of oral precancer. *Oral Oncol* **49**, 1129–35 (2013).
30. Zhang, L., Poh, C. F., Williams, M., Laronde, D. M., Berean, K. & Gardner, P. J. et al. Loss of Heterozygosity (LOH) Profiles–Validated Risk Predictors for Progression to Oral Cancer. *Cancer Prev Res* **5**, 1081–9 (2012).
31. Fonseca-Silva, T., Diniz, M. G., De Sousa, S. F., Gomez, R. S. & Gomes, C. C. Association between histopathological features of dysplasia in oral leukoplakia and loss of heterozygosity. *Histopathology* **68**, 456–60 (2016).
32. Regezi, J. A., Zarbo, R. J., Regev, E., Pisanty, S., Silverman, S. & Gazit, D. p53 protein expression in sequential biopsies of oral dysplasias and in situ carcinomas. *J Oral Pathol Med* **24**, 18–22 (1995).
33. Kushner, J., Bradley, G. & Jordan, R. C. Patterns of p53 and Ki-67 protein expression in epithelial dysplasia from the floor of the mouth. *J Pathol* **183**, 418–23 (1997).
34. Rowley, H., Helliwell, T. R., Jones, A. S., Roland, N. J., Field, E. A. & Field, J. K. An immunohistochemical analysis of p53 protein expression in pre-malignant and malignant tissues of the oral cavity. *Clin Otolaryngol Allied Sci* **22**, 23–29 (1997).
35. Kurokawa, H., Matsumoto, S., Murata, T., Yamashita, Y., Tomoyose, T. & Zhang, M. et al. Immunohistochemical study of syndecan-1 down-regulation and the expression of p53 protein or Ki-67 antigen in oral leukoplakia with or without epithelial dysplasia. *J Oral Pathol Med* **32**, 513–21 (2003).

36. Kohda, M., Tokuzawa, Y., Kishita, Y., Nyuzuki, H., Moriyama, Y. & Mizuno, Y. et al. A comprehensive genomic analysis reveals the genetic landscape of mitochondrial respiratory chain complex deficiencies. *PLoS Genet* **12**, e1005679 (2016).
37. Bolger, A. M., Lohse, M. & Usadel, B. Trimmomatic: a flexible trimmer for Illumina sequence data. *Bioinformatics* **30**, 2114–20 (2014).
38. Li, H. & Durbin, R. Fast and accurate short read alignment with Burrows-Wheeler transform. *Bioinformatics* **25**, 1754–60 (2009).
39. Li, H., Handsaker, B., Wysoker, A., Fennell, T., Ruan, J. & Homer, N. et al. The sequence alignment/map format and SAMtools. *Bioinformatics* **25**, 2078–9 (2009).
40. McKenna, A., Hanna, M., Banks, E., Sivachenko, A., Cibulskis, K. & Kernytsky, A. et al. The Genome Analysis Toolkit: A MapReduce framework for analyzing next-generation DNA sequencing data. *Genome Res* **20**, 1297–303 (2010).
41. Wilm, A., Aw, P. P. K., Bertrand, D., Yeo, G. H. T., Ong, S. H. & Wong, C. H. et al. LoFreq: a sequence-quality aware, ultra-sensitive variant caller for uncovering cell-population heterogeneity from high-throughput sequencing datasets. *Nucleic Acids Res* **40**, 11189–201 (2012).
42. Gravitt, P. E., Peyton, C. L., Alessi, T. Q., Wheeler, C. M., Coutlee, F. & Hildesheim, A. et al. Improved amplification of genital human papillomaviruses. *J Clin Microbiol* **38**, 357–61 (2000).
43. Fuessel Haws, A. L., He, Q., Rady, P. L., Zhang, L., Grady, J. & Hughes, T. K. et al. Nested PCR with the PGMY09/11 and GP5(+)/6(+) primer sets improves detection of HPV DNA in cervical samples. *J Virol Methods* **122**, 87–93 (2004).
44. Erhart, S. M., Rivero, E. R., Bazzo, M. L. & Onofre, A. S. Comparative evaluation of the GP5+/6+, MY09/11 and PGMY09/11 primer sets for HPV detection by PCR in oral squamous cell carcinomas. *Exp Mol Pathol* **100**, 13–16 (2016).
45. Xu-Monette, Z. Y., Wu, L., Visco, C., Tai, Y. C., Tzankov, A. & Liu, W.-M. et al. Mutational profile and prognostic significance of TP53 in diffuse large B-cell lymphoma patients treated with R-CHOP: report from an International DLBCL Rituximab-CHOP Consortium Program Study. *Blood* **120**, 3986–96 (2012).
46. Soong, D., Stratford, J., Avet-Loiseau, H., Bahlis, N., Davies, F. & Dispenzieri, A. et al. CNV Radar: an improved method for somatic copy number alteration characterization in oncology. *BMC Bioinform* **21**, 98 (2020).
47. Kanda, Y. Investigation of the freely available easy-to-use software 'EZR' for medical statistics. *Bone Marrow Transpl* **48**, 452–8 (2013).
48. Kastenhuber, E. R. & Lowe, S. W. Putting p53 in Context. *Cell* **170**, 1062–78 (2017).
49. Woo, S.-B., Grammer, R. L. & Lerman, M. A. Keratosis of unknown significance and leukoplakia: a preliminary study. *Oral Surg Oral Med Oral Pathol Oral Radio* **118**, 713–24 (2014).
50. Holmstrup, P., Vedtofte, P., Reibel, J. & Stoltze, K. Long-term treatment outcome of oral premalignant lesions. *Oral Oncol* **42**, 461–74 (2006).
51. Napier, S. S. & Speight, P. M. Natural history of potentially malignant oral lesions and conditions: an overview of the literature. *J Oral Pathol Med* **37**, 1–10 (2008).
52. Cruz, I. B., Snijders, P. J., Meijer, C. J., Braakhuis, B. J., Snow, G. B. & Walboomers, J. M. et al. p53 expression above the basal cell layer in oral mucosa is an early event of malignant transformation and has predictive value for developing oral squamous cell carcinoma. *J Pathol* **184**, 360–8 (1998).
53. Viveka, T. S., Shyamsundar, V., Krishnamurthy, A., Ramani, P. & Ramshankar, V. p53 expression helps identify high risk oral tongue pre- malignant lesions and correlates with patterns of invasive tumour front and tumour depth in oral tongue squamous cell carcinoma cases. *Asian Pac J Cancer Prev* **17**, 189–95 (2016).
54. Horne, G. M., Anderson, J. J., Tiniakos, D. G., McIntosh, G. G., Thomas, M. D. & Angus, B. et al. p53 protein as a prognostic indicator in breast carcinoma: a comparison of four antibodies for immunohistochemistry. *Br J Cancer* **73**, 29–35 (1996).
55. Lavieille, J. P., Righini, C., Reyt, E., Brambilla, C. & Riva, C. Implications of p53 alterations and anti-p53 antibody response in head and neck squamous cell carcinomas. *Oral Oncol* **34**, 84–92 (1998).
56. Villa, A., Hanna, G. J., Kacew, A., Frustino, J., Hammerman, P. S. & Woo, S. B. Oral keratosis of unknown significance shares genomic overlap with oral dysplasia. *Oral Dis* **25**, 1707–14 (2019).
57. Köbel, M., Piskorz, A. M., Lee, S., Lui, S., LePage, C. & Marass, F. et al. Optimized p53 immunohistochemistry is an accurate predictor of TP53 mutation in ovarian carcinoma. *J Pathol Clin Res* **2**, 247–58 (2016).
58. Yemelyanova, A., Vang, R., Kshirsagar, M., Lu, D., Marks, M. A. & Shih, I. M. et al. Immunohistochemical staining patterns of p53 can serve as a surrogate marker for TP53 mutations in ovarian carcinoma: an immunohistochemical and nucleotide sequencing analysis. *Mod Pathol* **24**, 1248–53 (2011).
59. Liu, Y., Chen, C., Xu, Z., Scuoppo, C., Rillahan, C. D. & Gao, J. et al. Deletions linked to TP53 loss drive cancer through p53-independent mechanisms. *Nature* **531**, 471–5 (2016).

ACKNOWLEDGEMENTS

We thank Ms. Kazuko Matsuno, Kyoko Kiuchi, Yuko Ohno, Tomohiro Aoki, and Kumiko Osawa for their technical assistance. The authors received no specific funding for this work.

AUTHOR CONTRIBUTIONS

K.S., S.M., M.H. and JI.T. designed and performed the research, analyzed and interpreted data, and wrote the paper. K.S., S.M., R.K. and T.I. performed the pathological review of the cases. K.S., S.M. and R.K. provided the study material or patients. M.K., K.M. and Y.O. provided technical support. T.K. and N.H. supervised the assembly of the clinical data. All authors read and approved the final paper.

COMPETING INTERESTS

The authors declare no competing interests.

ETHICS APPROVAL

The present study was approved by the Institutional Review Board of Saitama Medical Center (No 1967) and conducted in accordance with the Declaration of Helsinki.

ADDITIONAL INFORMATION

Supplementary information The online version contains supplementary material available at https://doi.org/10.1038/s41379-021-00893-9.

Correspondence and requests for materials should be addressed to S.M.

Reprints and permission information is available at http://www.nature.com/reprints

Publisher's note Springer Nature remains neutral with regard to jurisdictional claims in published maps and institutional affiliations.